

MOLECULAR HYDROGEN FORMATION ON ASTROPHYSICALLY RELEVANT SURFACES

N. KATZ,¹ I. FURMAN,¹ O. BIHAM,¹ V. PIRRONELO,² AND G. VIDALI³

Received 1999 January 22; accepted 1999 April 23

ABSTRACT

Recent experimental results about the formation of molecular hydrogen on astrophysically relevant surfaces under conditions close to those encountered in the interstellar medium are analyzed using rate equations. The parameters of the rate equation model are fitted to temperature-programmed desorption curves obtained in the laboratory. These parameters are the activation energy barriers for atomic hydrogen diffusion and desorption, the barrier for molecular hydrogen desorption, and the probability of spontaneous desorption of a hydrogen molecule upon recombination. The model is a generalization of the Polanyi-Wigner equation and provides a description of both first- and second-order kinetic processes within a single model. Using the values of the parameters that best fit the experimental results, the efficiency of hydrogen recombination on olivine and amorphous carbon surfaces is obtained for a range of hydrogen flux and surface temperature pertinent to a wide range of interstellar conditions.

Subject headings: dust, extinction — ISM: abundances — ISM: molecules — molecular processes

1. INTRODUCTION

The formation of molecular hydrogen in the interstellar medium (ISM) is a process of fundamental importance (Duley & Williams 1984; Williams 1998). It was recognized long ago (Gould & Salpeter 1963) that H_2 cannot form in the gas phase efficiently enough to account for its abundance. It was proposed that dust grains act as catalysts allowing the protomolecule to quickly release the 4.5 eV of excess energy in a time comparable to the vibration period of the highly vibrationally excited state in which it is formed. The problem can be described as follows. An H atom approaching the surface of a grain has a probability ξ of becoming adsorbed. The adsorbed H atom (adatom) spends an average time t_H (residence time) before leaving the surface. If during the residence time the H adatom encounters another H adatom, an H_2 molecule will form with a certain probability.

This problem has been studied theoretically over the years, and different models have been proposed (Gould & Salpeter 1963; Williams 1968; Hollenbach & Salpeter 1970, 1971; Hollenbach, Werner, & Salpeter 1971; Smoluchowski 1981, 1983; Aronowitz & Chang 1985; Duley & Williams 1986; Pirronello & Aversa 1988; Sandford & Allamandola 1993; Takahashi, Masuda, & Nagaoka 1999; Farebrother, Fisher, & Clary 1999). In particular, Hollenbach et al. (1971) calculated sticking and accommodation of H atoms in a semiclassical way, while the mobility was treated quantum mechanically. They concluded that tunneling between adsorption sites, even at 10 K, would have ensured the required mobility. The steady state production rate of molecular hydrogen per unit volume was expressed according to (Hollenbach et al. 1971)

$$R_{H_2} = \frac{1}{2} n_H v_H \sigma \gamma n_g, \quad (1)$$

where n_H and v_H are the number density and the speed of H atoms in the gas phase, respectively, σ is the average cross-sectional area of a grain, and n_g is the number density of

dust grains. The parameter γ is the fraction of H atoms striking the grain that eventually form a molecule, namely, $\gamma = \xi \eta$, where η is the probability that an H adatom on the surface will recombine with another H atom to form H_2 . The probability ξ for an H atom to become adsorbed on a grain surface covered by an ice mantle has been calculated by Buch & Zhang (1991) and Masuda, Takahashi, & Mukai (1998). Equation (1) states that, for $\eta = 1$, whenever two H atoms are adsorbed on a grain, a H_2 molecule is formed.

Recently a series of experiments was conducted to measure hydrogen recombination in an ultra-high-vacuum (UHV) chamber by irradiating the sample with two beams of H and D atoms and monitoring the HD production rate (Pirronello et al. 1997a, 1997b, 1999). The two beams were used in order to obtain a better signal-to-noise ratio than would have been possible for H_2 . Two different substrates have been used: a natural olivine (a silicate made of a mixture of Mg_2SiO_4 and Fe_2SiO_4) slab, and an amorphous carbon sample. These samples are considered better analogs of interstellar dust than any model surface studied before. The substrate temperatures were in the range between 5 and 15 K. The HD formation rate was measured using a quadrupole mass spectrometer both *during* and *after* irradiation with H and D atoms. In the latter case, a temperature programmed desorption (TPD) experiment was carried out in which the temperature of the sample was quickly ramped to over 30 K to desorb all weakly adsorbed species.

The main results obtained by Pirronello et al. (1997a, 1997b, 1999) are as follows: (1) In the temperature range of interest for interstellar applications (between 10 and 15 K), the formation rates deduced from the experimental data are about an order of magnitude lower than those calculated by Hollenbach & Salpeter (1970, 1971) and Hollenbach et al. (1971). (2) According to the desorption spectra, hydrogen, that is adsorbed as atomic appears to acquire significant mobility only around 9 K in the case of olivine and at a somewhat higher temperature in the case of amorphous carbon, even in the high-coverage regime. Thus, at temperatures lower than about 10 K tunneling alone does not provide enough mobility to H adatoms to enable recombination, and thermal activation is required.

In this paper we perform a detailed analysis of the hydrogen recombination experiments of Pirronello et al. (1997a,

¹ Racah Institute of Physics, Hebrew University of Jerusalem, Jerusalem 91904, Israel.

² Istituto di Fisica, Università di Catania, 95125 Catania, Sicily, Italy.

³ Department of Physics, Syracuse University, Syracuse, NY 13244.

1997b, 1999) using a rate equation model. The parameters of the rate equation model are fitted to the experimental TPD curves. These parameters are the activation energy barriers for atomic hydrogen diffusion and desorption, the barrier for molecular hydrogen desorption, and the probability of spontaneous desorption of a hydrogen molecule upon recombination. Using the values of the parameters that best fit the experimental results, the efficiency of hydrogen recombination on the olivine and amorphous carbon surfaces is obtained for a range of hydrogen fluxes and surface temperatures pertinent to a wide range of interstellar conditions.

The paper is organized as follows. In § 2 we describe the experiments to be analyzed. The rate equation model is introduced in § 3. Subsequent analysis and results are presented in § 4, followed by a discussion in § 5 and a summary in § 6.

2. REVIEW OF EXPERIMENTAL METHODS

The experimental apparatus and measurement techniques are described in Pirronello et al. (1997a, 1997b, 1999) and in greater detail in Vidali et al. (1998a). Here we give a brief outline. The apparatus consists of an ultra-high-vacuum chamber pumped by a cryopump and a turbomolecular pump (operating pressure in the low 10^{-10} torr range). The sample is placed in the center of the UHV chamber and mounted on a liquid helium continuous flow cryostat. By varying the flow of liquid helium and with the use of a heater located behind the sample, temperatures can be maintained in the range of 5–30 K. For cleaning purposes, the temperature of the sample can be raised to about 200°C (without liquid helium in the cryostat). The temperature is measured by an iron-gold/chromel thermocouple and a calibrated silicon diode placed in contact with the sample. Two triple differentially pumped atomic beam lines are aimed at the surface of the sample. Each has a radio-frequency cavity in which the molecular species is dissociated, cooled to ~ 200 K by passing the atoms through a cooled Al channel, and then injected into the line. Dissociation rates are typically in the 75%–90% range, and are constant throughout a run. Estimated fluxes are as low as 10^{12} atoms $\text{cm}^{-2} \text{s}^{-1}$ (Vidali et al. 1998a).

The reason for using two different lines and two isotopes (one line for H and the other for D) is that in preliminary runs using only one line, it became evident that the signal of H_2 formation was hidden in the background given by the undissociated fraction of molecules coming directly from the beam source. The possibility of using a second line is undoubtedly one of the most important features of this equipment. By using H atoms in one line and D atoms in the other, we can look at the formation of HD on the surface, knowing that there are no other spurious sources of HD. The signal of HD is collected by a quadrupole mass spectrometer mounted on a rotatable flange. The experiment is done in two phases. First, H and D beams are sent onto the surface for a given period of time (from tens of seconds to tens of minutes). At this time any HD formed and released is detected. In the second phase (the TPD phase), the sample temperature is quickly ($\sim 0.6 \text{ K s}^{-1}$) ramped and the HD signal is measured.

By measuring the desorption rate $R(t)$ as a function of time, as well as the temperature of the surface as a function of time, information on the kinetics of desorption can be obtained. The desorption rate can be approximated by the

Polanyi-Wigner equation:

$$R(t) = \nu N(t)^\beta \exp(-E_d/k_B T), \quad (2)$$

where N is the number density of reactants on the surface, β is the order of desorption, ν is the attempt frequency, E_d is the effective activation energy for the dominant recombination and desorption process, and $T = T(t)$ is the sample temperature. In the TPD experiment, first-order ($\beta = 1$) desorption curves $R(t)$ exhibit asymmetric peaks with a sharp dropoff on the right-hand side. The position of the peak is insensitive to coverage. Second-order desorption curves ($\beta = 2$) exhibit symmetric peak shapes. These peaks shift toward lower temperatures as coverage is increased (Chan, Aris, & Weinberg 1978).

In the experiments analyzed here the irradiation stage was done at a surface temperature between $T = 5$ and $T = 7$ K, for several irradiation time intervals. The HD desorption rate versus surface temperature during the TPD runs is shown in Figures 1 and 2 for olivine and in Figures 3 and 4 for amorphous carbon. The TPD curves shown in Figures 1 and 3 exhibit first-order kinetics due to the larger irradiation times, while the ones shown in Figures 2 and 4 exhibit second-order kinetics. For both the olivine and the amorphous carbon samples, at the sample temperature examined here, most of the HD detected is formed because of thermal activation during the heat pulse. Only a small fraction of HD is formed during the irradiation process, showing that, at least under our experimental conditions, prompt-reaction mechanisms (Duley & Williams 1986) and fast tunneling (Hollenbach et al. 1971) are not that important.

3. MODEL

3.1. Assumptions

In the desorption curves studied here most of the adsorbed hydrogen is released well before a temperature of 30 K is reached. Therefore, we assume that the hydrogen atoms on the surface are trapped in physisorption potential wells and are thus only weakly adsorbed. We also assume that the mechanism for the creation of H_2 (or HD) is the Langmuir-Hinshelwood (LH) scheme, namely, that the rate of creation of H_2 is diffusion limited. This assumption is justified because of the observed Langmuir-like kinetics of the amounts desorbed as a function of the irradiation time (Pirronello et al. 1997b). Since the coverages involved in the experiments analyzed here are low, other mechanisms such as the Eley-Rideal (ER) scheme, in which hydrogen atoms, coming from the gas phase, collide and promptly react with already adsorbed hydrogen atoms, are of less importance and are not included in our model. Furthermore, the experimental results indicate that the ER mechanism does not contribute significantly, since even at higher coverages there was little desorption of HD during the irradiation phase.

The model we present here reproduces quite well the experimental desorption curves, and the choices of the assumptions on which it is based are the results of other less successful attempts. We have, in fact, tried to fit the desorption curves using a model in which the H and D populations of adatoms that are used in the experiments were described separately. In these earlier attempts we assumed that all HD molecules are promptly released upon formation, as investigations on more regular metal surfaces suggest (Rettner & Auerbach 1996; Winkler 1998). The

model in that case has four parameters: the diffusion barriers as well as the desorption barriers for H and D adatoms. We found that such a model cannot provide a reasonable fit to the experimental desorption curves.

In the model we present here, we do not assume spontaneous desorption once a molecule is created on the surface despite the ~ 4.5 eV released in the recombination. In order not to increase the number of parameters to be used in the fits, we decided not to treat separately the two populations of H and D adatoms, but to consider only one population of H adatoms characterized by average properties. In this way we kept the number of parameters to four: the activation energy barriers for diffusion and desorption of hydrogen adatoms, the activation energy barrier for desorption of molecular hydrogen that had not been released into the gas phase upon formation, and the probability $1 - \mu$ of spontaneous desorption of a hydrogen molecule upon recombination.

An important final assumption is that all energy barriers are coverage independent. This assumption may not apply at high coverage. However, at the low coverages obtained in the experiments analyzed here (up to $\sim 1\%$ of a layer), it is a reasonable assumption.

3.2. Rate Equations

Consider an experiment in which a flux of H atoms is irradiated on the surface. H atoms that stick to the surface, once the surface temperature is raised, perform hops as random walkers with increased frequency and recombine when they encounter one another. Let $N_1(t)$ (in monolayers [ML]) be the coverage of H atoms on the surface and $N_2(t)$ (also in ML) the coverage of H₂ molecules. We obtain the following set of rate equations:

$$\dot{N}_1 = F(1 - N_1 - N_2) - P_1 N_1 - 2\alpha N_1^2, \quad (3a)$$

$$\dot{N}_2 = \mu\alpha N_1^2 - P_2 N_2. \quad (3b)$$

The first term on the right-hand side of equation (3a) represents the incoming flux in the Langmuir kinetics. In this scheme H atoms deposited on top of H atoms or H₂ molecules already on the surface are rejected. F represents an *effective* flux (in units of ML s⁻¹); that is, it already includes the possibility of a temperature-dependent sticking coefficient. The second term in equation (3a) represents the desorption of H atoms from the surface. The desorption coefficient is

$$P_1 = \nu \exp(-E_1/k_B T), \quad (4)$$

where ν is the attempt rate (it is standard to take this as 10^{12} s⁻¹), E_1 is the activation energy barrier for desorption of an H atom, and T is the temperature. The third term in equation (3a) accounts for the depletion of the H population on the surface due to recombination into H₂ molecules, where

$$\alpha = \nu \exp(-E_0/k_B T) \quad (5)$$

is the hopping rate of H atoms on the surface and E_0 is the activation energy barrier for H diffusion. Here we assume that there is no barrier for recombination. If such a barrier is considered, it can be introduced as discussed in Pirronello et al. (1997a, 1999). The first term on the right-hand side of equation (3b) represents the creation of H₂ molecules. The factor 2 in the third term of equation (3a) does not appear here, since it takes two H atoms to form one molecule. The

parameter μ represents the fraction of H₂ molecules that remains on the surface upon formation, while a fraction of $(1 - \mu)$ is spontaneously desorbed because of the excess energy released in the recombination process. The second term in equation (3b) describes the desorption of H₂ molecules. The desorption coefficient is

$$P_2 = \nu \exp(-E_2/k_B T), \quad (6)$$

where E_2 is the activation energy barrier for H₂ desorption. The H₂ production rate R is given by

$$R = (1 - \mu)\alpha N_1^2 + P_2 N_2. \quad (7)$$

This model can be considered as a generalization of the Polanyi-Wigner model (see eq. [2]). It gives rise to a wider range of simultaneous applications, compared to equation (2). In particular, it describes both first-order and second-order desorption kinetics (or a combination) for different regimes of temperature and flux.

In the experiments analyzed here, both the temperature and the flux were controlled and monitored throughout. Each experiment consists of two phases. In the first phase the sample temperature is constant up to time t_0 , under a constant irradiation rate F_0 . In the second phase, the irradiation is turned off and linear heating of the sample is applied at the rate b (K s⁻¹):

$$F(t) = F_0: \quad T(t) = T_i, \quad 0 \leq t < t_0, \quad (8)$$

$$F(t) = 0: \quad T(t) = T_i + b(t - t_0), \quad t \geq t_0. \quad (9)$$

Here T_i is the constant temperature of the sample during irradiation.

In the case that the rejection terms in $F(1 - N_1 - N_2)$ are neglected and the effective flux becomes simply F (a valid assumption at low coverages), the rate equations can be solved analytically. However, the solution is expressed in terms of intractable nested integral expressions, and is of little use to us. In the case we study here, in which the rejection terms are taken into account, no such solution exists and the equations are integrated numerically.

4. ANALYSIS AND RESULTS

4.1. Methods

We will now examine to what extent the rate equation model can describe the experimental results. To this end we performed numerical integration of equations (3a) and (3b) with the aid of a Bulirsch-Stoer stepper algorithm (Press et al. 1992). The result of the integration is a set of TPD curves that are a function of the chosen set of parameters. A standard TPD experimental run includes the time dependence of the flux $F(t)$ and temperature $T(t)$ as well as the four parameters E_0 , E_1 , E_2 and μ . The temperature $T(t)$ is measured directly via a thermocouple. The flux $F(t)$ (s⁻¹) is estimated as described elsewhere (Vidali et al. 1998b). An approximate value for $F(t)$, in the required units of ML s⁻¹, can be obtained by integrating the TPD spectra, generating the total *yield* of the various experiments. The flux is then obtained from the exponential fit indicated by Langmuir kinetics. It is important to stress that this is a lower bound value for the flux, and this value is reached only if there is no H desorption at all. We are now left with the four parameters E_0 , E_1 , E_2 , and μ , which are assumed to be independent of the flux or temperature. These parameters form a four-dimensional space that has to be explored in order to

find the values for which the calculated TPD curves provide the best fit to the experimental ones.

The merit function to be minimized in the fitting procedure is the standard χ^2 function, which is the sum over the squares of the differences between the experimental points and the calculated ones. Another possibility that we considered was to compare the derivatives of the experimental TPD curves with those of the simulation (again using χ^2). This possibility required using the Savitzki-Golay filtering (Press et al. 1992) in order to obtain a reasonably smooth derivative from the experimental data, because of the well-known increase in the noise-to-signal ratio in any derivative of measured data.

To obtain the parameters that best fit the experimental data, one needs to probe the parameter space and find the set of values of the parameters that give rise to the global minimum of the merit function. The probing procedure we used is based on random search. A point in the four-dimensional parameter space is randomly picked. A numerical integration of the model's equations is performed with the chosen parameters. The merit function obtained from the comparison of the resulting curve with the experimental curve is then evaluated. If this set represents an improvement over the current minimum, the new point is accepted as the new minimum. If, however, the new set did not score lower (i.e., better) than the known minimum, it was promptly discarded. The probability distribution for picking the next random set of parameters was taken to be a Lorentzian centered around the current set of parameters, and thus favored nearby points. The relatively slow dropoff of the Lorentzian function also allowed the occasional taking of longer steps and thus prevented the process from getting stuck in a local minimum.

4.2. Results

The experimental TPD curves and the fits obtained by the rate equations are shown in Figures 1 and 2 for the olivine sample and in Figures 3 and 4 for the amorphous carbon sample. The parameters obtained in the fitting procedure for the two samples are shown in Table 1. The parameter set generated for each sample represents a simultaneous best fit for all the six TPD curves. Fitting each curve separately typically produces better fits, but at the expense of an increased range in the values of the parameters. These variations allow us to generate approximate error estimates. It is found that the energy barriers E_0 and E_2 are very well determined by this process (to within several tenths of a meV). The barrier E_1 is not as well determined, and its values given above, for both samples, are to be taken as lower bounds to the correct value (within 3 meV). The parameter μ is determined to within ± 0.1 , and

thus justifies our assumption, within this model, that not all H_2 molecules immediately desorb upon recombination. Attempting to artificially force $\mu = 0$ and do the fits with the remaining three parameters, degrades the fit substantially and cannot recreate the entire range of behavior of the data simultaneously.

Although equation (2) can be used to fit the entire range of experimental TPD results, this equation, which includes a single activation energy, does not provide as much insight as our model (eqs. [3a] and [3b]). For example, applying equation (2) in the case of Figure 1 (olivine; first-order desorption kinetics), we use $\beta = 1$ and arrive at $E_d = 26.8$ meV. This is equivalent to the E_2 found for olivine using this model. However, as we shift to Figure 2 (olivine; second-order desorption kinetics), we must now take $\beta = 2$, which results in $E_d = 24$ meV. Here the rate-limiting process is the diffusion on the surface, and therefore E_d is closer to E_0 . Unlike equation (2), our model does not require setting a parameter (such as β). Furthermore, it provides the best-fit values of each of the relevant activation energies for both the first- and second-order kinetics and using the same framework.

The model (eqs. [3a] and [3b]) can also describe the steady state conditions that are reached when both the flux and the temperature are fixed. The steady state solution is then easily obtained by setting \dot{N}_1 and \dot{N}_2 to zero and solving the quadratic equation for N_1 . The coefficients P_1 , P_2 , and α in the rate equations are temperature dependent and under the steady state assumption maintain constant values. The complete solution under these assumptions takes the form (after neglecting the unphysical possibility of the negative root)

$$N_1 = \frac{[(P_1 + F)^2 + 8(\alpha F + \mu \alpha F^2/2P_2)]^{1/2}}{4(\alpha F + \mu \alpha F^2/2P_2)} - \frac{P_1 + F}{4(\alpha F + \mu \alpha F^2/2P_2)}, \quad (10a)$$

$$N_2 = \frac{(P_1 + F)^2 + 4(\alpha F + \mu \alpha F^2/2P_2)}{8(\alpha + \mu \alpha F/2P_2)^2} - \frac{(P_1 + F)[(P_1 + F)^2 + 8(\alpha F + \mu \alpha F^2/2P_2)]^{1/2}}{8(\alpha + \mu \alpha F/2P_2)^2}. \quad (10b)$$

Note that when the rejection terms in the flux are neglected, the expressions for the steady state coverages and recombination rate become significantly simpler (Biham et al. 1998). These solutions may be useful in the study of recombination processes in the interstellar medium where steady state conditions may be relevant.

In this work, we present a model that captures the kinetics of the diffusion-recombination-desorption process. The parameters thus obtained can then be used to study the astrophysically relevant cases. For example, by assuming steady state conditions, we can obtain the recombination efficiency as a function of flux F and temperature T for a range of parameters that goes from the astrophysically relevant (extremely low flux, 10–15 K) to the ones used in the laboratory (low flux, 5–30 K). The recombination efficiency is defined as the ratio between the production rate R (eq. [7]) and the deposition rate $F/2$ (in molecules).

Varying T and F over the astrophysically relevant range, we can identify the regions in which there is nonnegligible

TABLE 1

FOUR PARAMETERS OBTAINED BY FITTING TPD CURVES FOR POLYCRYSTALLINE OLIVINE AND AMORPHOUS CARBON^a

Material	E_0 (meV)	E_1 (meV)	E_2 (meV)	μ
Olivine	24.7	32.1	27.1	0.33
Amorphous carbon	44.0	56.7	46.7	0.413

^a E_0 is the barrier for atomic diffusion, E_1 and E_2 are the barriers for atomic and molecular desorption, respectively, and $1 - \mu$ is the probability of spontaneous desorption of a newly formed H_2 molecule.

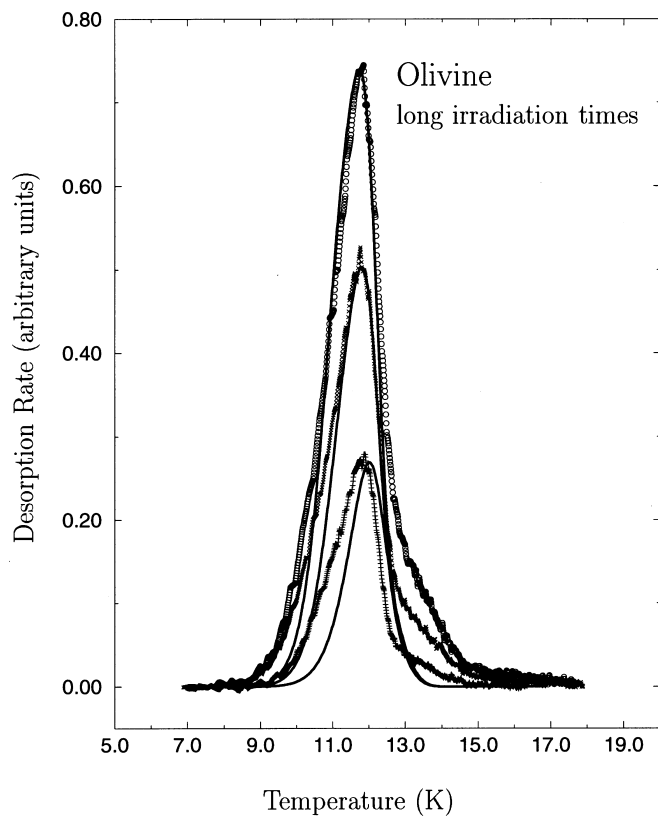


FIG. 1.—TPD curves for higher coverage experiments on an olivine slab. Irradiation times (in minutes) are 8.0 (*circles*), 5.5 (*crosses*), and 2.0 (*plus signs*). Fits are shown by solid lines.

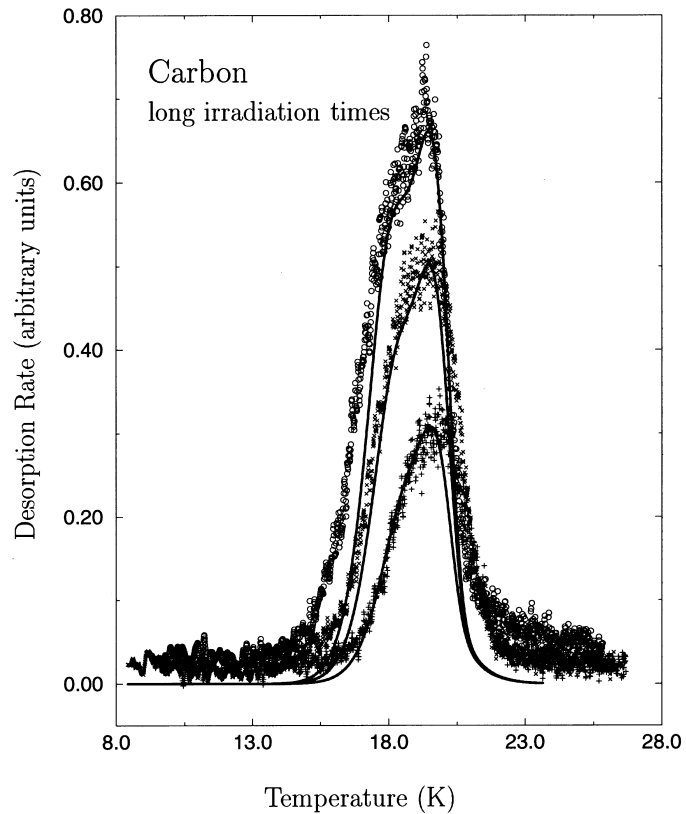


FIG. 3.—TPD curves for higher coverage experiments on amorphous carbon. Irradiation times (in minutes) are 32.0 (*circles*), 16.0 (*crosses*), and 8.0 (*plus signs*). Fits are shown by solid lines.

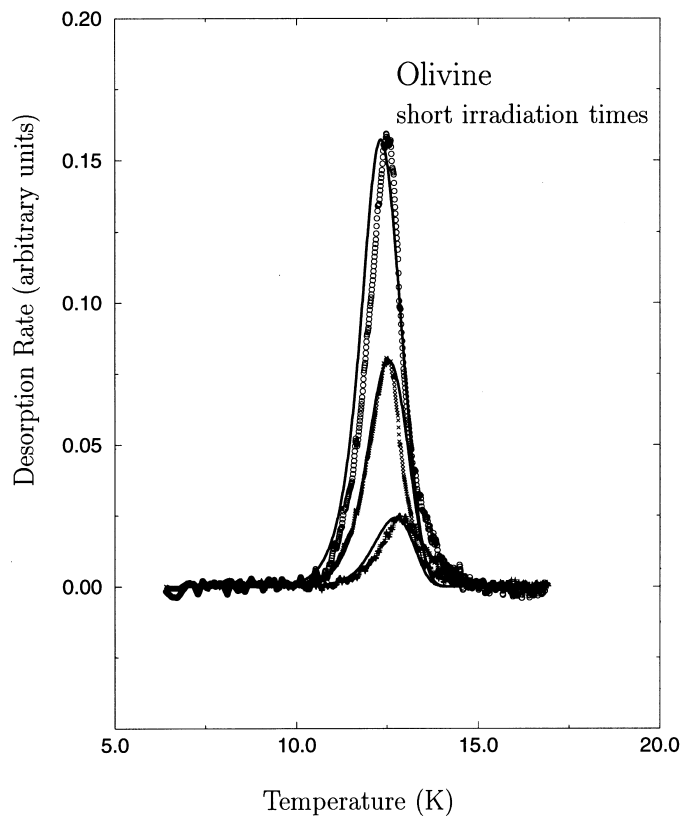


FIG. 2.—TPD curves for lower coverage experiments on an olivine slab. Irradiation times (in minutes) are 0.55 (*circles*), 0.2 (*crosses*), and 0.07 (*plus signs*). Fits are shown by solid lines.

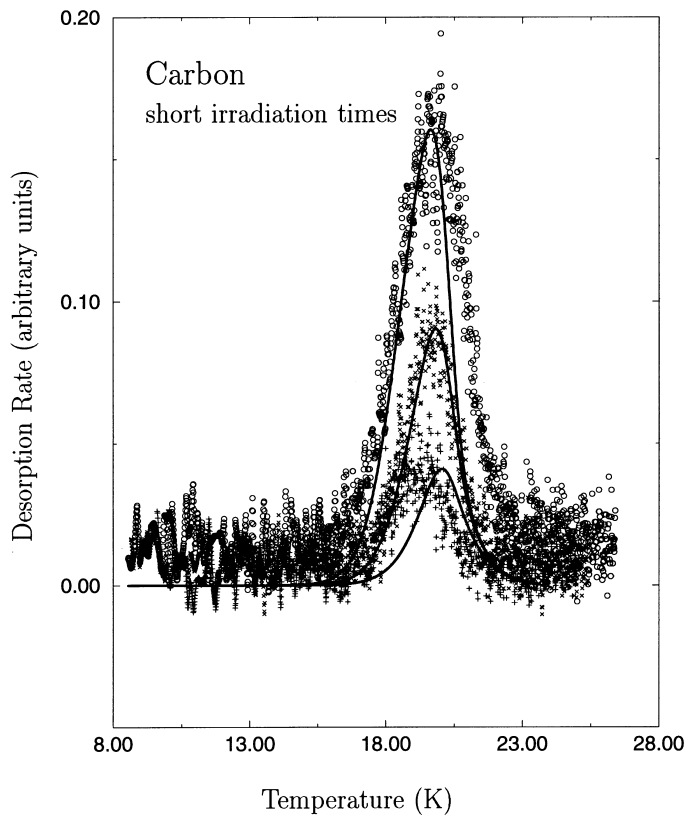


FIG. 4.—TPD curves for lower coverage experiments on amorphous carbon. Irradiation times (in minutes) are 4.0 (*circles*), 2.0 (*crosses*), and 1.0 (*plus signs*). Fits are shown by solid lines.

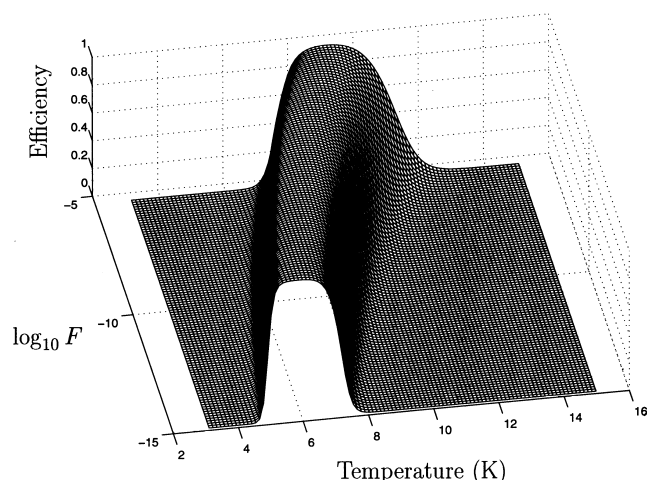


FIG. 5.—Recombination efficiency at steady state of the olivine slab as a function of $\log_{10} F$ (flux in ML s^{-1}) and T (temperature in K).

recombination efficiency. The recombination efficiency as a function of T and F is shown in Figure 5 for olivine and in Figure 6 for amorphous carbon. The main conclusion from these figures is that the recombination efficiency is highly temperature dependent. There is an efficiency window along the temperature axis which shifts to higher temperatures as the flux is increased. It is found that under astrophysically relevant irradiation rates the efficiency for olivine drops off at approximately 7–8 K, while for amorphous carbon it drops off only at 13–14 K.

We find that, for both samples, the parameter μ (the probability that an H_2 molecule will remain on the surface upon recombination) has little effect on the production rate R of molecular hydrogen under steady state conditions. This is easy to understand, since under steady state conditions the production rate R must be equal to the recombination rate on the surface, and, thus, must be independent of μ . The coverage of hydrogen molecules on the surface is adjusted accordingly. Similarly, the energy barrier for desorption of molecular hydrogen, E_2 , has little effect on the recombination efficiency, under steady state conditions,

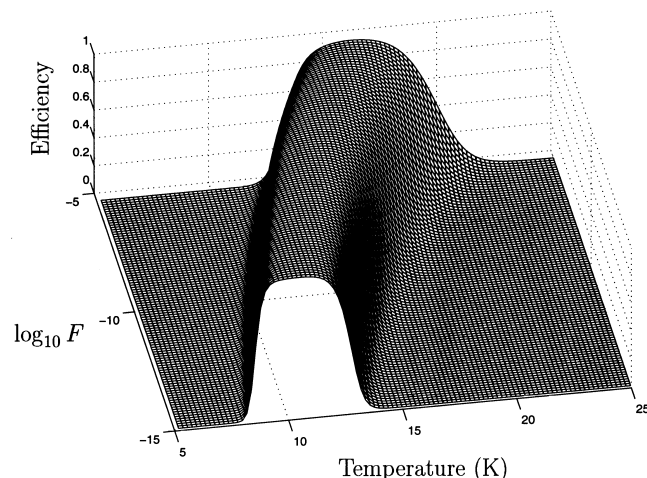


FIG. 6.—Recombination efficiency at steady state of amorphous carbon as a function of $\log_{10} F$ (flux in ML s^{-1}) and T (temperature in K).

as long as it remains significantly smaller than the barrier for atomic desorption, E_1 .

5. DISCUSSION

Amorphous materials in general, and their surfaces in particular, are difficult to characterize, owing to their irregular structure and composition. In the experiments analyzed here, this difficulty gives rise to some uncertainty about the role of quantum effects. In principle, tunneling of H atoms should be considered. However, the experiments indicate that quantum effects appear to be small, as the mobility of the hydrogen atoms is very low at the lower irradiation temperatures (Pirronello et al. 1997a). Another issue is that in the experiments the desorption rates of HD were measured and the extrapolation to processes involving H and H_2 is nontrivial. This difficulty is unavoidable, however, owing to the large background noise in the measurements of H_2 production. Careful calibration of the apparatus was used in generating the necessary extrapolation coefficients. Taking isotopic effects into account in the rate equations is not easy for this type of surface, since the shape of the energy surface is not known. An attempt was made to introduce separate fitting parameters for H and D, while keeping $\mu = 0$ (to maintain the same number of parameters). This fit was considerably worse than the ones presented here. Since isotopic effects enter as a shift in the activation energies of the various processes described here, it is fair to consider an “effective” hydrogen atom in the simulations.

Despite these obstacles, we obtained good fits to the experimental TPD curves using numerical integration of the rate equation model. This seems to indicate that most of the processes that occur at the microscopic level are captured by the dynamics of the rate equations, or at least they average out to this global dynamics.

According to common physical intuition based on long-range forces and the values of atomic and molecular polarizabilities, H_2 is expected to be bound to the substrate more tightly than H. This, however, does not appear to be the case: the parameters calculated numerically, for both samples, put the H atoms in deeper wells than H_2 . This feature must signal the fact that more complicated interactions (based also on shorter range forces) are taking place.

The recombination efficiency diagrams (Figs. 5–7) include two regions of low efficiency on both sides of the high-efficiency window. The asymptotic steady state coverage in the region on the left-hand side approaches unity, while everywhere else it is very small. This is due to the fact that at such low temperatures atoms remain stuck in place and barely diffuse; thus recombination is inhibited. These atoms accumulate on the surface, blocking adsorption sites (“Langmuir rejection”). However, this high coverage regime is not one that we can extrapolate to with any certainty within this rate equation model. As already suggested in Pirronello et al. (1999), mechanisms such as Eley-Rideal or diffusion by tunneling, which are not taken into account in the model, may become significant in this regime. Nevertheless, we can speculate that if the Langmuir rejection remains significant even at higher coverages, the trend in recombination efficiency shown should remain qualitatively correct. Luckily, such low temperatures are rarely of astrophysical interest. For olivine, at temperatures above 6.5 K, the calculated asymptotic coverage is very low and well within the regimes of experimentation and subsequent

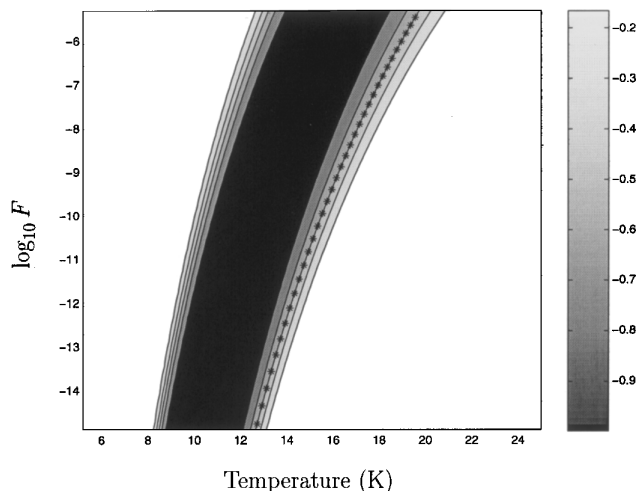


FIG. 7.—Contour plot of the recombination efficiency at steady state for amorphous carbon, as a function of $\log_{10} F$ (flux in ML s^{-1}) and T (temperature in K). The starred line represents $\alpha F = P_1^2$.

numerical simulation; consequently, the relevance of the model is justified.

We find that the recombination efficiency on olivine is high in the temperature range of roughly 5–10 K; however, this temperature range is lower than the one encountered in the interstellar clouds. Therefore, we believe that this material is not a very likely candidate for an efficient catalyst of hydrogen recombination in interstellar space.

The recombination efficiency on amorphous carbon, on the other hand, behaves differently (recall Fig. 6). Here we see that the final drop in efficiency of H₂ recombination is at higher temperatures, and amorphous carbon seems to be a more appropriate candidate of interstellar grains on which hydrogen may recombine with high efficiency.

In a previous paper (Biham et al. 1998) two limiting expressions were obtained for the H₂ production rate per unit volume under steady state conditions. Such expressions are linear (when $\alpha F \gg P_1^2$) or quadratic (when $\alpha F \ll P_1^2$) in the flux of gas-phase atoms. Alternatively, they are independent (when $\alpha F \gg P_1^2$) or quadratically dependent (when $\alpha F \ll P_1^2$) on the coverage of H adatoms. Note that in Biham et al. (1998) the value $\mu = 1$ was taken. In that work we studied the steady state behavior of the rate equations for the processes described here, where the value of μ does not affect the recombination efficiency. The first of the two limits of the steady state production rate of molecular hydrogen per unit volume coincides with the expression of Hollenbach et al. (see eq. [1] above). However, it is found that the second of the two limits, which is valid when there is a very low coverage of H adatoms on interstellar grains, coincides with the expression proposed by Pirronello et al. (1997a):

$$R_{\text{H}_2} = (n_{\text{H}} v_{\text{H}} \sigma \xi t_{\text{H}})^2 n_{\text{g}} \alpha \gamma', \quad (11)$$

where $t_{\text{H}} = 1/P_1$ and γ' is the probability that two H adatoms recombine upon encountering (taking into account that there might be an activation energy for recombination).

In Figure 7 we present a contour diagram of the recombination efficiency on the carbon surface. On this diagram, the parameter values for which $\alpha F = P_1^2$ are plotted as a

starred line. In the region on the left-hand side of the starred line, the calculated R_{H_2} approaches the value obtained when $\alpha F \gg P_1^2$. On the right-hand side of the starred line, the calculated R_{H_2} approaches the value obtained in the limit of $\alpha F \ll P_1^2$. The transition from the regime where $\alpha F \gg P_1^2$ holds, to the other, where $\alpha F \ll P_1^2$, is quite rapid because of the exponential nature of the temperature dependence. We conclude that the two cases discussed in (Biham et al. 1998) apply in a wide region of the diagrams (Figs. 5–7).

The diagrams described above apply under conditions close to steady state. This is not necessarily the case in the interstellar clouds. If the entire cloud is far from steady state, one must return to the original rate equation model and take into account the time dependence of the flux and temperature.

The values obtained for μ imply a nonnegligible probability for the hydrogen molecules to remain on the surface instead of being immediately ejected into the gas phase. This result was found to be unavoidable within the assumption of the model used here. There are various mechanisms for efficient heat transfer from the molecule to the surface. These may dissipate the excess energy and prevent immediate desorption. One possible mechanism may be due to the very irregular structure of the sample surfaces: olivine was mechanically polished (hence there should be grooves of hundreds of angstroms in width and depth). Atomic force microscopy (AFM) images of the olivine surface show such a rugged landscape at the submicron scale, while amorphous carbon is composed of grains of the size of ~ 100 angstroms. A definite possibility (more relevant in the amorphous carbon case, as the somewhat larger μ -value suggests) is that hydrogen molecules, even if promptly released upon formation, do not necessarily go directly into the vacuum but undergo a series of collisions in which part of their energy is released to the solid with a subsequent readsorption. Such mechanism was identified for H and D atoms impinging on an amorphous ice particle (Buch & Zhang 1991). More experiments are needed in order to elucidate the nature of the recombination process at the atomic scale and to obtain a value for μ directly.

6. SUMMARY

Experimental results on the formation of molecular hydrogen on various materials under conditions relevant to interstellar clouds were analyzed using rate equations. By fitting the results of a TPD experiment to a rate equation model, four essential parameters of the process were obtained. These are the activation energy barriers for atomic hydrogen diffusion and desorption, the barrier for molecular hydrogen desorption, and the probability of spontaneous desorption of a hydrogen molecule upon recombination. The results compare favorably with what is obtained from the Polanyi-Wigner equation. Furthermore, the model represents a generalization that allows us to describe both first- and second-order processes (or even a combination of the two) within a single model.

In this work we have shown a procedure to extrapolate data taken under conditions available in the laboratory to values that should hold in astrophysical environments, and to determine the efficiency of various surfaces as catalysts in molecule production. Polycrystalline olivine was shown to be inefficient as a catalyst in the relevant temperature/flux regime. On amorphous carbon a higher efficiency was

reached due to higher desorption/diffusion barriers that cause a rise in the recombination efficiency at the relevant temperatures.

The proposed model and methods of analysis are neither complete nor definitive; nonetheless they represent a serious improvement over what has been used so far to

predict the behavior of hydrogen on astrophysically relevant surfaces.

G. V. acknowledges support from NASA grant NAG5-6822.

REFERENCES

- Aronowitz, S., & Chang, S. 1985, *ApJ*, 293, 243
 Biham, O., Furman, I., Katz, N., Pirronello, V., & Vidali, G. 1998, *MNRAS*, 296, 869
 Buch, V., & Zhang, Q. 1991, *ApJ*, 379, 647
 Chan, C. M., Aris, R., & Weinberg, W. H. 1978, *Appl. Surf. Sci.*, 1, 360
 Duley, W. W., & Williams, D. A. 1984, *Interstellar Chemistry* (London: Academic)
 ———. 1986, *MNRAS*, 223, 177
 Farebrother, A., Fisher, A., & Clary, D. C. 1999, in preparation
 Gould, R. J., & Salpeter, E. E. 1963, *ApJ*, 138, 393
 Hollenbach, D., & Salpeter, E. E. 1970, *J. Chem. Phys.*, 53, 79
 ———. 1971, *ApJ*, 163, 155
 Hollenbach, D., Werner, M. W., & Salpeter, E. E. 1971, *ApJ*, 163, 165
 Masuda, K., Takahashi, J., & Mukai, T. 1998, *A&A*, 330, 773
 Pirronello, V., & Averna, D. 1988, *A&A*, 201, 196
 Pirronello, V., Biham, O., Liu, C., Shen, L., & Vidali, G. 1997a, *ApJ*, 483, L131
 Pirronello, V., Liu, C., Roser, J. E., & Vidali, G. 1999, *A&A*, in press
 Pirronello, V., Liu, C., Shen, L., & Vidali, G. 1997b, *ApJ*, 475, L69
 Press, W. H., Teukolsky, S. A., Vetterling, W. T., & Flannery, B. P. 1992, *Numerical Recipes in C: The Art of Scientific Computing* (Cambridge: Cambridge Univ. Press)
 Rettner, C. T., & Auerbach, D. J. 1996, *Surf. Sci.*, 357, 602
 Sandford, S. A., & Allamandola, L. J. 1993, *ApJ*, 409, L65
 Smoluchowski, R. 1981, *Ap&SS*, 75, 353
 ———. 1983, *J. Phys. Chem.*, 87, 4229
 Takahashi, J., Masuda, K., & Nagaoka, M. 1999, *A&A*, in press
 Vidali, G., Pirronello, V., Liu, C., & Shen, L. Y. 1998a, *Astrophys. Lett. Commun.*, 35, 423
 Vidali, G., Roser, J., Liu, C., Pirronello, V., & Biham, O. 1998b, in *Proc. NASA Lab. Space Sci. Workshop* (Cambridge: CfA), 60
 Williams, D. A. 1968, *ApJ*, 151, 935
 ———. 1998, *Faraday Disc.* 109, 1
 Winkler, A. 1998, *Appl. Phys. A*, 67, 637